# Boiling of nuclear liquid in the micro-canonical ensemble

K. Miyazaki

E-mail: miyazakiro@rio.odn.ne.jp

**Abstract**

New calculus of the liquid-gas phase transition is developed for the boiling of nuclear liquid in the micro-canonical ensemble. In contrast to the familiar geometrical construction, the temperature and the chemical potentials are determined from definite values of baryon densities and pressure. We recover the concave maximized entropy in the phase transition against the common tangent filling up the convex intruder. Consequently, the caloric curve reproduces the experimental data well.

The asymmetric nuclear matter is a binary system that has two independent chemical potentials of proton and neutron. In nuclear liquid-gas phase transition [1-4] both the chemical potentials in the liquid and gaseous phases are equilibrated according to the Gibbs condition on the phase equilibrium. In many theoretical works [5-10] they are determined via the geometrical construction. One of the prominent signals of nuclear liquid-gas phase transition is the plateau on the caloric curve [11,12] found in nuclear multifragmentation reactions. In calculating the caloric curve of nuclear matter, the temperature and the chemical potentials should be determined simultaneously from definite values of the other thermodynamic quantities. In this sense the object in our study is the micro-canonical ensemble. Nevertheless, the chemical potentials in the geometrical construction are calculated for a definite value of temperature. Although our previous work [13] investigated the caloric curve in the micro-canonical ensemble of nuclear matter, we used the Maxwell construction for phase equilibrium. It is not appropriate to binary system. On the other hand, we have recently succeeded [14] in constructing the liquid-gas phase transition in a pure canonical ensemble of asymmetric nuclear matter against the neutron grand-canonical but proton canonical ensemble in Ref. [15]. Then, in the present paper we extend the calculus developed in Ref. [14] to the micro-canonical ensemble of asymmetric nuclear matter.

Our basis is the relativistic mean-field model of nuclear matter developed in Refs. [13] and [16]. It can reproduce the recent astronomical observations of neutron stars, the density-dependence of the nuclear symmetry energy and the critical temperature of symmetric nuclear matter. In the model, at finite temperature $T$, the thermodynamic potential per volume $\tilde{\Omega} \equiv \Omega/V$ of asymmetric nuclear matter is given by

$$\begin{aligned}\tilde{\Omega} &= \frac{1}{2} m_\sigma^2 \langle\sigma\rangle^2 + \frac{1}{2} m_\delta^2 \langle\delta_3\rangle^2 - \frac{1}{2} m_\omega^2 \langle\omega_0\rangle^2 - \frac{1}{2} m_\rho^2 \langle\rho_{03}\rangle^2 \\ &\quad - \gamma\, k_B T \sum_{i=p,n} \int_0^\infty \frac{d^3\mathbf{k}}{(2\pi)^3} \left\{ \ln\left[1 + \exp\left(\frac{\nu_i - E_{ki}^*}{k_B T}\right)\right] + \ln\left[1 + \exp\left(\frac{-\nu_i - E_{ki}^*}{k_B T}\right)\right]\right\},\end{aligned} \tag{1}$$

where $k_B$ is the Boltzmann constant and $\gamma = 2$ is the spin-isospin degeneracy. $E_{ki}^* = (\mathbf{k}^2 + M_i^{*2})^{1/2}$ is the energy of a nuclear nucleon, which is a quasi-particle of the effective mass $M_i^* = m_i^* M_N = M_N + S_i$ in the scalar potential $S_i$. The $\nu_i$ is defined using the chemical potential $\mu_i$ and the vector potential $V_i = v_i\, M_N$ as

$$\nu_i = \mu_i - V_i. \tag{2}$$

The self-consistent equations [13] to determine the effective masses and the vector potentials of proton and neutron are obtained by extremizing $\tilde{\Omega}$. For calculating the caloric curve of nuclear matter, we have to specify the pressure $P = -\tilde{\Omega}$, the total baryon density

$$\rho_B = \rho_{Bp} + \rho_{Bn}, \tag{3}$$

and the asymmetry

$$a = \frac{\rho_{Bn} - \rho_{Bp}}{\rho_B}. \tag{4}$$

The resultant 7th-rank nonlinear simultaneous equations are solved so that the effective masses, the vector potentials, the chemical potentials and the temperature are determined. In this sense the object in our study is the micro-canonical ensemble. We have calculated the entropy per baryon $S/A$ as a function of the enthalpy per baryon $H/A$ under the constant pressure $P = 0.03\text{MeV/fm}^3$ and the definite asymmetry $a = 0.3$. The detailed calculational procedure is the same as that in Ref. [13]. The result is the black curve in Fig. 1. A dip or a convex intruder between $H/A = 3.76$MeV and 31.2MeV is due to the liquid-gas phase transition. Although the asymmetric nuclear matter is the binary system, we can draw the common tangent shown by the red line so as to fill up the dip.

Figure 2 shows the caloric curve of nuclear matter, the temperature $T$ as a function of the excitation energy per baryon $E^*/A$. (We assume $k_B = 1$.) The triangles are the experimental data from the multifragmentation reaction of Fig. 5 in Ref. [13]. The numerical result shown by the black curve cannot reproduce them. We can see that the data above $E^*/A = 6$MeV approximately lie on the horizontal line of $T \simeq 8$MeV. The result is just a observational signal of nuclear liquid-gas phase transition. From the common tangent in Fig. 1, via $\partial S/\partial H = 1/T$, we derive the boiling temperature $T = 8.25$MeV of nuclear liquid shown by the red line. The temperature is also determined from a crossing point on the black curve in Fig. 3, which shows the Gibbs energy per baryon as a function of temperature.

In detail the experimental caloric curve increases gradually below $E^*/A = 6$MeV. The red line from the common tangent cannot reproduce the result. This is because it is a signal of binary nature $\mu_p \neq \mu_n$ of asymmetric nuclear matter, while the common tangent prescription is reasonable only for symmetric nuclear matter. So as to resolve the problem, we have to reproduce the liquid-gas mixed phase to satisfy the Gibbs condition on the phase equilibrium in asymmetric nuclear matter. For the purpose we will calculate the following 12th-rank simultaneous nonlinear equations. The four equations of them determine the effective masses and the vector potentials of proton and neutron in the gaseous phase marked with suffix $g$:

$$\begin{aligned}\frac{\partial\,\tilde{\Omega}}{\partial\,M_p^{(g)*}} = \rho_{Sp}^{(g)} + m_\sigma^2\,\frac{\langle\sigma\rangle_g}{M_N}\,\frac{\partial\,\langle\sigma\rangle_g}{\partial\,m_p^{(g)*}} + m_\delta^2\,\frac{\langle\delta_3\rangle_g}{M_N}\,\frac{\partial\,\langle\delta_3\rangle_g}{\partial\,m_p^{(g)*}} & \\ -\,m_\omega^2\,\frac{\langle\omega_0\rangle_g}{M_N}\,\frac{\partial\,\langle\omega_0\rangle_g}{\partial\,m_p^{(g)*}} - m_\rho^2\,\frac{\langle\rho_{03}\rangle_g}{M_N}\,\frac{\partial\,\langle\rho_{03}\rangle_g}{\partial\,m_p^{(g)*}} &= 0,\end{aligned}\tag{5}$$

$$\begin{aligned}\frac{\partial\,\tilde{\Omega}}{\partial\,V_p^{(g)}} = \rho_{Bp}^{(g)} + m_\sigma^2\,\frac{\langle\sigma\rangle_g}{M_N}\,\frac{\partial\,\langle\sigma\rangle_g}{\partial\,v_p^{(g)}} + m_\delta^2\,\frac{\langle\delta_3\rangle_g}{M_N}\,\frac{\partial\,\langle\delta_3\rangle_g}{\partial\,v_p^{(g)}} & \\ -\,m_\omega^2\,\frac{\langle\omega_0\rangle_g}{M_N}\,\frac{\partial\,\langle\omega_0\rangle_g}{\partial\,v_p^{(g)}} - m_\rho^2\,\frac{\langle\rho_{03}\rangle_g}{M_N}\,\frac{\partial\,\langle\rho_{03}\rangle_g}{\partial\,v_p^{(g)}} &= 0,\end{aligned}\tag{6}$$

$$\begin{aligned}\frac{\partial\,\tilde{\Omega}}{\partial\,M_n^{(g)*}} = \rho_{Sn}^{(g)} + m_\sigma^2\,\frac{\langle\sigma\rangle_g}{M_N}\,\frac{\partial\,\langle\sigma\rangle_g}{\partial\,m_n^{(g)*}} + m_\delta^2\,\frac{\langle\delta_3\rangle_g}{M_N}\,\frac{\partial\,\langle\delta_3\rangle_g}{\partial\,m_n^{(g)*}} & \\ -\,m_\omega^2\,\frac{\langle\omega_0\rangle_g}{M_N}\,\frac{\partial\,\langle\omega_0\rangle_g}{\partial\,m_n^{(g)*}} - m_\rho^2\,\frac{\langle\rho_{03}\rangle_g}{M_N}\,\frac{\partial\,\langle\rho_{03}\rangle_g}{\partial\,m_n^{(g)*}} &= 0,\end{aligned}\tag{7}$$

$$\begin{aligned}\frac{\partial\,\tilde{\Omega}}{\partial\,V_n^{(g)}} = \rho_{Bn}^{(g)} + m_\sigma^2\,\frac{\langle\sigma\rangle_g}{M_N}\,\frac{\partial\,\langle\sigma\rangle_g}{\partial\,v_n^{(g)}} + m_\delta^2\,\frac{\langle\delta_3\rangle_g}{M_N}\,\frac{\partial\,\langle\delta_3\rangle_g}{\partial\,v_n^{(g)}} & \\ -\,m_\omega^2\,\frac{\langle\omega_0\rangle_g}{M_N}\,\frac{\partial\,\langle\omega_0\rangle_g}{\partial\,v_n^{(g)}} - m_\rho^2\,\frac{\langle\rho_{03}\rangle_g}{M_N}\,\frac{\partial\,\langle\rho_{03}\rangle_g}{\partial\,v_n^{(g)}} &= 0.\end{aligned}\tag{8}$$

The explicit expressions of the mean-fields and their derivatives are given in Ref. [16].

Similarly, the equations for the liquid phase (marked with suffix $l$) are

$$
\begin{aligned}
\frac{\partial \tilde{\Omega}}{\partial M_p^{(l)*}} = \rho_{Sp}^{(l)} + m_\sigma^2 \frac{\langle \sigma \rangle_l}{M_N} \frac{\partial \langle \sigma \rangle_l}{\partial m_p^{(l)*}} + m_\delta^2 \frac{\langle \delta_3 \rangle_l}{M_N} \frac{\partial \langle \delta_3 \rangle_l}{\partial m_p^{(l)*}} \\
- m_\omega^2 \frac{\langle \omega_0 \rangle_l}{M_N} \frac{\partial \langle \omega_0 \rangle_l}{\partial m_p^{(l)*}} - m_\rho^2 \frac{\langle \rho_{03} \rangle_l}{M_N} \frac{\partial \langle \rho_{03} \rangle_l}{\partial m_p^{(l)*}} &= 0,
\end{aligned} \tag{9}
$$

$$
\begin{aligned}
\frac{\partial \tilde{\Omega}}{\partial V_p^{(l)}} = \rho_{Bp}^{(l)} + m_\sigma^2 \frac{\langle \sigma \rangle_l}{M_N} \frac{\partial \langle \sigma \rangle_l}{\partial v_p^{(l)}} + m_\delta^2 \frac{\langle \delta_3 \rangle_l}{M_N} \frac{\partial \langle \delta_3 \rangle_l}{\partial v_p^{(l)}} \\
- m_\omega^2 \frac{\langle \omega_0 \rangle_l}{M_N} \frac{\partial \langle \omega_0 \rangle_l}{\partial v_p^{(l)}} - m_\rho^2 \frac{\langle \rho_{03} \rangle_l}{M_N} \frac{\partial \langle \rho_{03} \rangle_l}{\partial v_p^{(l)}} &= 0,
\end{aligned} \tag{10}
$$

$$
\begin{aligned}
\frac{\partial \tilde{\Omega}}{\partial M_n^{(l)*}} = \rho_{Sn}^{(l)} + m_\sigma^2 \frac{\langle \sigma \rangle_l}{M_N} \frac{\partial \langle \sigma \rangle_l}{\partial m_n^{(l)*}} + m_\delta^2 \frac{\langle \delta_3 \rangle_l}{M_N} \frac{\partial \langle \delta_3 \rangle_l}{\partial m_n^{(l)*}} \\
- m_\omega^2 \frac{\langle \omega_0 \rangle_l}{M_N} \frac{\partial \langle \omega_0 \rangle_l}{\partial m_n^{(l)*}} - m_\rho^2 \frac{\langle \rho_{03} \rangle_l}{M_N} \frac{\partial \langle \rho_{03} \rangle_l}{\partial m_n^{(l)*}} &= 0,
\end{aligned} \tag{11}
$$

$$
\begin{aligned}
\frac{\partial \tilde{\Omega}}{\partial V_n^{(l)}} = \rho_{Bn}^{(l)} + m_\sigma^2 \frac{\langle \sigma \rangle_l}{M_N} \frac{\partial \langle \sigma \rangle_l}{\partial v_n^{(l)}} + m_\delta^2 \frac{\langle \delta_3 \rangle_l}{M_N} \frac{\partial \langle \delta_3 \rangle_l}{\partial v_n^{(l)}} \\
- m_\omega^2 \frac{\langle \omega_0 \rangle_l}{M_N} \frac{\partial \langle \omega_0 \rangle_l}{\partial v_n^{(l)}} - m_\rho^2 \frac{\langle \rho_{03} \rangle_l}{M_N} \frac{\partial \langle \rho_{03} \rangle_l}{\partial v_n^{(l)}} &= 0.
\end{aligned} \tag{12}
$$

The other two equations determine the mixture of gaseous and liquid phases in the phase transition:

$$
\rho_{Bp} = \frac{1}{2}(1-a)\,\rho_B = f_g\,\rho_{Bp}^{(g)} + \left(1 - f_g\right)\rho_{Bp}^{(l)}, \tag{13}
$$

$$
\rho_{Bn} = \frac{1}{2}(1+a)\,\rho_B = f_g\,\rho_{Bn}^{(g)} + \left(1 - f_g\right)\rho_{Bn}^{(l)}, \tag{14}
$$

where $0 \le f_g \le 1$ is the ratio of gas in the mixed phase. The baryon densities in gaseous and liquid phases are

$$
\rho_{Bi}^{(g)} = \gamma \int_0^\infty \frac{d^3\mathbf{k}}{(2\pi)^3} \left[ n_{ki}\left(m_i^{(g)*}, v_i^{(g)}; \mu_i, T\right) - \bar{n}_{ki}\left(m_i^{(g)*}, v_i^{(g)}; \mu_i, T\right) \right], \tag{15}
$$

$$
\rho_{Bi}^{(l)} = \gamma \int_0^\infty \frac{d^3\mathbf{k}}{(2\pi)^3} \left[ n_{ki}\left(m_i^{(l)*}, v_i^{(l)}; \mu_i, T\right) - \bar{n}_{ki}\left(m_i^{(l)*}, v_i^{(l)}; \mu_i, T\right) \right]. \tag{16}
$$

The scalar densities in Eqs. (5), (7), (9) and (11) are

$$
\rho_{Si}^{(g)} = \gamma \int_0^\infty \frac{d^3\mathbf{k}}{(2\pi)^3} \frac{M_i^{(g)*}}{E_{ki}^{(g)*}} \left[ n_{ki}\left(m_i^{(g)*}, v_i^{(g)}; \mu_i, T\right) + \bar{n}_{ki}\left(m_i^{(g)*}, v_i^{(g)}; \mu_i, T\right) \right], \tag{17}
$$

$$\rho_{Si}^{(l)} = \gamma \int_0^\infty \frac{d^3\mathbf{k}}{(2\pi)^3} \frac{M_i^{(l)*}}{E_{ki}^{(l)*}} \left[ n_{ki}\left(m_i^{(l)*}, v_i^{(l)}; \mu_i, T\right) + \bar{n}_{ki}\left(m_i^{(l)*}, v_i^{(l)}; \mu_i, T\right) \right]. \tag{18}$$

The Fermi-Dirac distribution functions of nucleon and antinucleon are

$$n_{ki}\left(m_i^*, v_i\,; \mu_i, T\right) = \left[1 + \exp\left(\frac{E_{ki}^* - \nu_i}{k_B T}\right)\right]^{-1}, \tag{19}$$

$$\bar{n}_{ki}\left(m_i^*, v_i\,; \mu_i, T\right) = \left[1 + \exp\left(\frac{E_{ki}^* + \nu_i}{k_B T}\right)\right]^{-1}. \tag{20}$$

We have performed the Fermi integral directly using the adaptive automatic integration with 20-points Gaussian quadrature.

The last two equations impose the equilibrium condition on pressures in the gaseous and liquid phases:

$$\begin{aligned} P &= \frac{1}{3\pi^2} \sum_{i=p,n} \int_0^\infty dk\, \frac{k^4}{E_{ki}^{(g)*}} \left[ n_{ki}\left(m_i^{(g)*}, v_i^{(g)}; \mu_i, T\right) + \bar{n}_{ki}\left(m_i^{(g)*}, v_i^{(g)}; \mu_i, T\right) \right] \\ &\quad - \frac{1}{2}\, m_\sigma^2 \left\langle \sigma \right\rangle_g^2 - \frac{1}{2}\, m_\delta^2 \left\langle \delta_3 \right\rangle_g^2 + \frac{1}{2}\, m_\omega^2 \left\langle \omega_0 \right\rangle_g^2 + \frac{1}{2}\, m_\rho^2 \left\langle \rho_{03} \right\rangle_g^2, \end{aligned} \tag{21}$$

$$\begin{aligned} P &= \frac{1}{3\pi^2} \sum_{i=p,n} \int_0^\infty dk\, \frac{k^4}{E_{ki}^{(l)*}} \left[ n_{ki}\left(m_i^{(l)*}, v_i^{(l)}; \mu_i, T\right) + \bar{n}_{ki}\left(m_i^{(l)*}, v_i^{(l)}; \mu_i, T\right) \right] \\ &\quad - \frac{1}{2}\, m_\sigma^2 \left\langle \sigma \right\rangle_l^2 - \frac{1}{2}\, m_\delta^2 \left\langle \delta_3 \right\rangle_l^2 + \frac{1}{2}\, m_\omega^2 \left\langle \omega_0 \right\rangle_l^2 + \frac{1}{2}\, m_\rho^2 \left\langle \rho_{03} \right\rangle_l^2. \end{aligned} \tag{22}$$

Solving Eqs. (5)-(14), (21) and (22) under definite values of pressure $P$ and baryon densities $\rho_{Bp}$ and $\rho_{Bn}$, we have the effective masses and the vector potentials of proton and neutron in each of phases, the chemical potentials of proton and neutron, the ratio of gaseous (or liquid) phase and the internal temperature of nuclear matter. In this sense the object in our study is the micro-canonical ensemble. For numerical calculations we have used the globally convergent Newton algorism in Ref. [17]. The trial values are easily found from the corresponding results in the common tangent prescription.

The blue dashed curve in Fig. 1 shows the entropy per baryon as a function of the enthalpy per baryon in the liquid-gas phase transition. The enthalpy per baryon is given by

$$\frac{H}{A} = \frac{\mathcal{E} + P}{\rho_B}. \tag{23}$$

The energy density is

$$\mathcal{E} = f_g\, \mathcal{E}_g + (1 - f_g)\, \mathcal{E}_l, \tag{24}$$

where the energy densities of gaseous and liquid phases in the phase transition are

$$\begin{aligned}\mathcal{E}_g &= \sum_{i=p,n}\int_0^\infty \frac{d^3\mathbf{k}}{(2\pi)^3}E_{ki}^{(g)*}\left[n_{ki}\left(m_i^{(g)*},v_i^{(g)};\mu_i,T\right)+\bar{n}_{ki}\left(m_i^{(g)*},v_i^{(g)};\mu_i,T\right)\right]\\ &+\sum_{i=p,n}V_i^{(g)}\rho_{Bi}^{(g)}+\frac{1}{2}m_\sigma^2\left\langle\sigma\right\rangle_g^2+\frac{1}{2}m_\delta^2\left\langle\delta_3\right\rangle_g^2-\frac{1}{2}m_\omega^2\left\langle\omega_0\right\rangle_g^2-\frac{1}{2}m_\rho^2\left\langle\rho_{03}\right\rangle_g^2, \quad (25)\end{aligned}$$

$$\begin{aligned}\mathcal{E}_l &= \sum_{i=p,n}\int_0^\infty \frac{d^3\mathbf{k}}{(2\pi)^3}E_{ki}^{(l)*}\left[n_{ki}\left(m_i^{(l)*},v_i^{(l)};\mu_i,T\right)+\bar{n}_{ki}\left(m_i^{(l)*},v_i^{(l)};\mu_i,T\right)\right]\\ &+\sum_{i=p,n}V_i^{(l)}\rho_{Bi}^{(l)}+\frac{1}{2}m_\sigma^2\left\langle\sigma\right\rangle_l^2+\frac{1}{2}m_\delta^2\left\langle\delta_3\right\rangle_l^2-\frac{1}{2}m_\omega^2\left\langle\omega_0\right\rangle_l^2-\frac{1}{2}m_\rho^2\left\langle\rho_{03}\right\rangle_l^2. \quad (26)\end{aligned}$$

The entropy per baryon is calculated in terms of the Gibbs-Duhem relation

$$T\,\frac{S}{A}=\frac{H-G}{A}, \quad (27)$$

where the Gibbs energy per baryon is

$$\frac{G}{A}=\frac{\mu_p\,\rho_{Bp}+\mu_n\,\rho_{Bn}}{\rho_B}. \quad (28)$$

We can see that the Gibbs condition on the phase equilibrium leads to the entropy being larger than the common tangent because the Gibbs condition is derived from the maximization of entropy. It is also seen that the region of phase transition between the two blue dots (between $H/A = 1.85$MeV and 32.1MeV) is wider than the one between the two red dots from the common tangent because the entropy should be concave. The concavity produces the graduate increase of temperature in the phase transition against the constant temperature from the common tangent. Consequently, the caloric curve, the blue curve in Fig. 2, reproduces the experimental data well. Here the excitation energy per baryon is defined by subtracting the binding energy of cold ($T = 0$) asymmetric nuclear matter [16] from $\mathcal{E}/\rho_B$.

We see in Fig. 3 that the maximum entropy leads to the minimum Gibbs energy (the blue dashed curve) in the phase transition between the two blue dots. The temperatures on the left and right dots are just the boiling temperature $T = 5.82$MeV of nuclear liquid and the condensed temperature $T = 8.77$MeV of nuclear gas, respectively. Then, we investigate both the temperatures for the other asymmetries than $a = 0.3$. The results are shown by the blue and red curves in Fig. 4. It is seen from the dotted lines that the nuclear liquid of asymmetry $a = 0.3$ begins to evaporate into highly asymmetric nuclear gas of $a_g = \frac{\left(\rho_{Bn}^{(g)}-\rho_{Bp}^{(g)}\right)}{\left(\rho_{Bn}^{(g)}+\rho_{Bp}^{(g)}\right)} = 0.988$, which is almost composed of neutrons. When the evaporation completes, the liquid phase is in rather symmetric state of asymmetry

$a_l = \frac{\left(\rho_{Bn}^{(l)} - \rho_{Bp}^{(l)}\right)}{\left(\rho_{Bn}^{(l)} + \rho_{Bp}^{(l)}\right)} = 0.057.$

We have developed a new calculus of the liquid-gas phase transition in the microcanonical ensemble of asymmetric nuclear matter based on the relativistic mean-field model in Refs. [15] and [16]. It is different from the geometrical construction used widely in the literature. The temperature and the chemical potentials are determined from definite values of baryon densities and pressure. The resultant entropy is maximized and so lies above the common tangent, while the Gibbs energy is minimized. Because of the concavity of the entropy, the temperature increases slowly in the phase transition from liquid to gas. Consequently, the caloric curve calculated for appropriate values of asymmetry and pressure reproduces the experimental data well. We also investigate the change of asymmetry in the gaseous and liquid phases during the boiling process. In a future work we will extend the present calculus to nuclear system in the nonextensive statistics.

# References


[1] J. Richert and P. Wagner, Phys. Rep. **350** (2001) 1 [arXiv:nucl-th/0009023].

[2] S.D. Gupta, A.Z. Mekjian and M.B. Tsang, *Advances in Nuclear Physics*, Vol. **26** (Kluwer Academic, 2001) [arXiv:nucl-th/0009033].

[3] V.E. Viola *et al.*, Phys. Rep. **434** (2006) 1 [arXiv:nucl-ex/0604012].

[4] V.A. Karnaukhov, Phys. Elem. Part. Atom. Nucl. **37** (2006) 312 [http://www1.jinr.ru/Pepan/Pepan_index.html].

[5] H. Műller and B.D. Serot, Phys. Rev. C **52** (1995) 2072 [arXiv:nucl-th/9505013].

[6] W.L. Qian, R-K. Su and P. Wang, Phys. Lett. B **491** (2000) 90 [arXiv:nucl-th/0008057].

[7] P.K. Panda, G. Klein, D.P. Menezes and C. Providência, Phys. Rev. C **68** (2003) 015201 [arXiv:nucl-th/0306045].

[8] P. Wang, D.B. Leinweber, A.W. Thomas and A.G. Williams, Nucl. Phys. A **748** (2005) 226 [arXiv:nucl-th/0407057].

[9] J. Xu, L-W. Chen, B-A. Li and H-R. Ma, arXiv:nucl-th/0702085.

[10] V.M. Kolomietz, A.I. Sanzhur, S. Shlomo and S.A. Firin, Phys. Rev. C **64** (2001) 024315 [arXiv:nucl-th/0104013].

[11] J.B. Natowitz *et al.*, Phys. Rev. C **65** (2002) 034618 [arXiv:nucl-ex/0106016].

[12] A. Ruangma *et al.*, Phys. Rev. C **66** (2002) 044603.

[13] K. Miyazaki, Mathematical Physics Preprint Archive (mp_arc) 07-64.

[14] K. Miyazaki, Mathematical Physics Preprint Archive (mp_arc) 07-92.

[15] C. Ducoin, Ph. Chomaz and F. Gulminelli, Nucl. Phys. A **771** (2006) 68 [arXiv:nucl-th/0512029].

[16] K. Miyazaki, Mathematical Physics Preprint Archive (mp_arc) 06-336.

[17] W.H. Press, S.A. Teukolsky, W.T. Vetterling and B.P. Flannery, Numerical Recipes in C 2nd edition, 1992, Cambridge University Press [http://www.nr.com/].

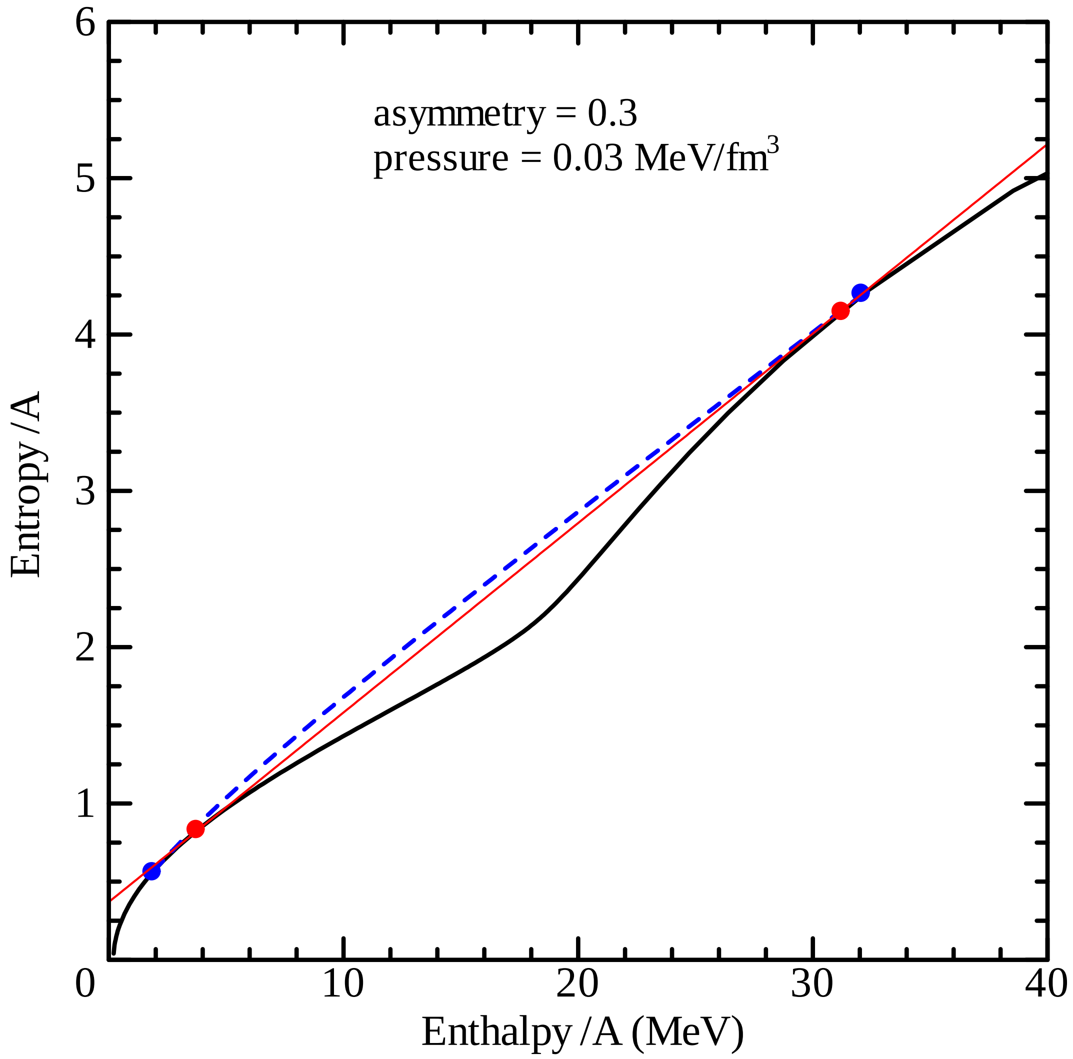


Figure 1: The black curve is the entropy per baryon as a function of the enthalpy per baryon for asymmetric nuclear matter of asymmetry $a = 0.3$ and pressure $P = 0.03\mathrm{MeV/fm}^3$. The red line is the common tangent that contacts with the black curve on the two red dots. The blue dashed curve between the two blue dots is the maximized entropy satisfying the Gibbs condition on the liquid-gas phase equilibrium.

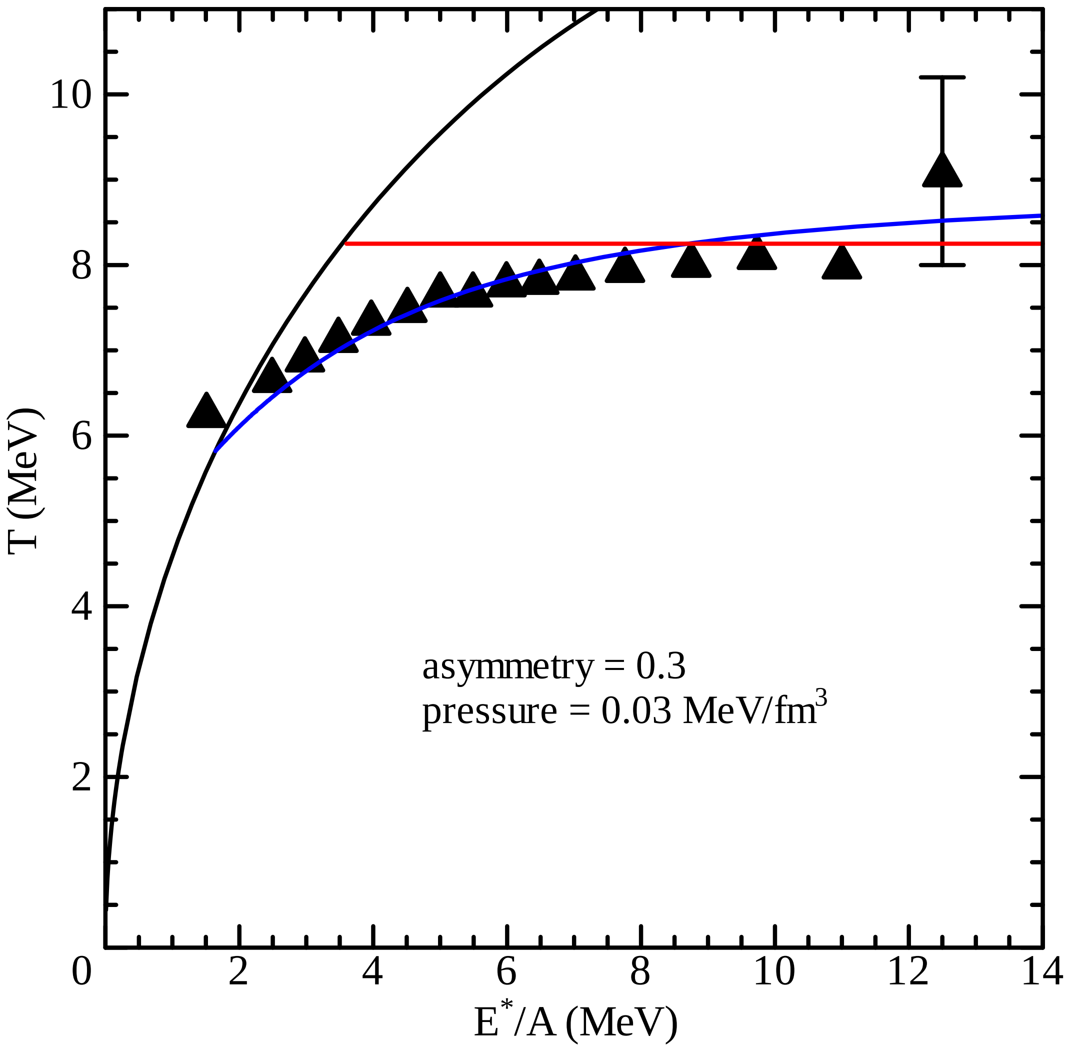


Figure 2: The black curve is the caloric curve derived from the black curve in Fig. 1. The horizontal red line is the constant temperature in the liquid-gas phase transition from the common tangent in Fig. 1. The blue curve is the caloric curve in the phase transition derived from the blue dashed curve in Fig. 1. The triangles are the experimental data from Fig. 5 in Ref. [13].

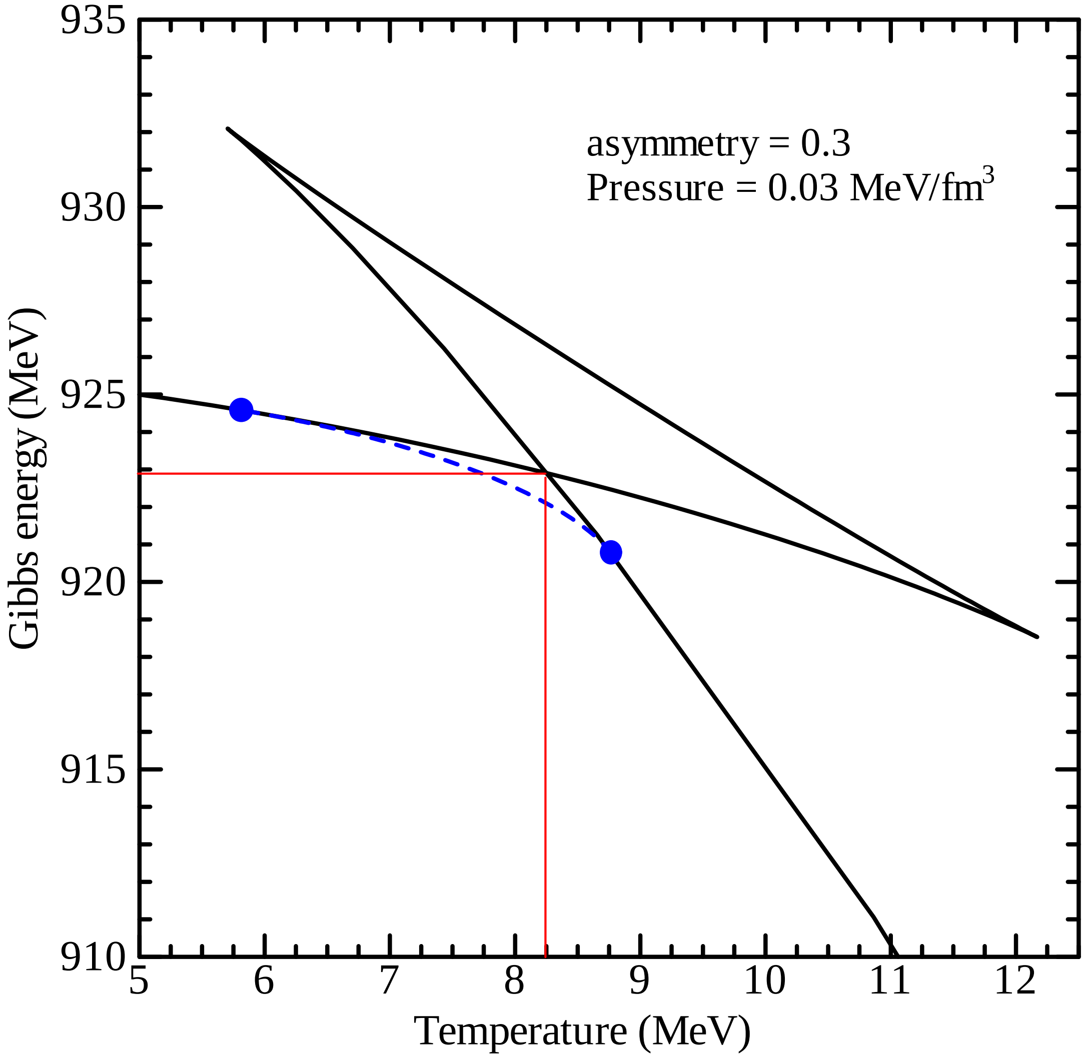


Figure 3: The Gibbs energy per baryon as a function of temperature for $a = 0.3$ and $P = 0.03\mathrm{MeV/fm}^3$. The black curve is the value corresponding to the black curve in Fig. 1. It has a crossing point denoted by the red line. The blue dashed curve between the two blue dots is the Gibbs energy in the liquid-gas phase transition, which satisfies the Gibbs condition on the phase equilibrium in asymmetric nuclear matter.

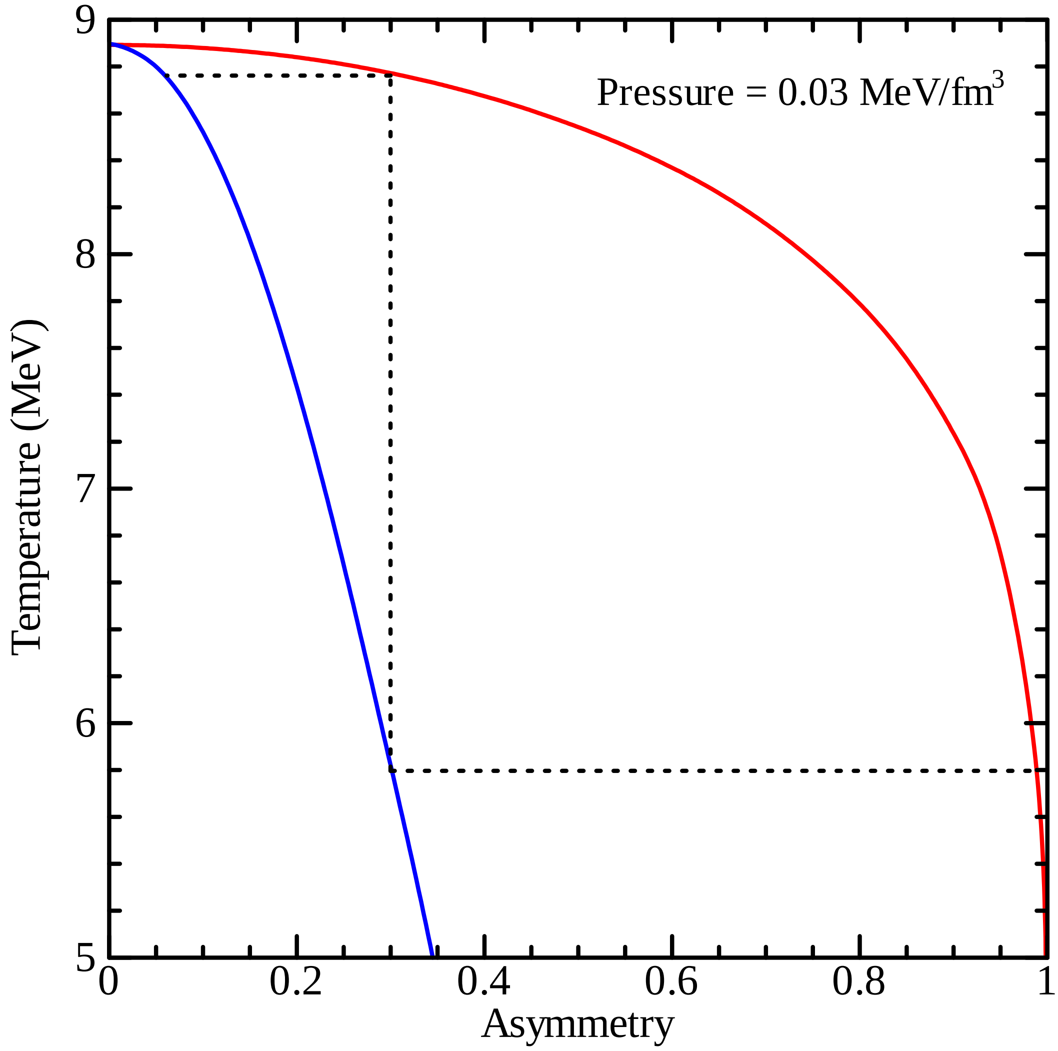


Figure 4: The boiling (blue) and condensed (red) curves of nuclear liquid and gas under the constant pressure $P = 0.03\mathrm{MeV/fm^3}$. The dotted lines show the boiling process in nuclear liquid of asymmetry $a = 0.3$.